J Therm Anal Calorim (2010) 101:919–924
DOI 10.1007/s10973-009-0504-7

On the thermal degradation of 3-methylaminopropylamine captured inside the aluminum phosphate analog of ULM-3

Nevenka Rajic · Djordje Stojakovic · Sanja Jevtic · Natasa Zabukovec Logar · Gregor Mali · Venceslav Kaucic

Received: 31 August 2009 / Accepted: 17 September 2009 / Published online: 27 October 2009

Abstract An open-framework aluminophosphate analog of the fluorogallophosphate structure-type ULM-3 was obtained by hydrothermal crystallization of an aqueous aluminum phosphate suspension in the presence of 3-methylpropylamine (MAPA) and hydrofluoric acid. The open-framework fluorinated aluminophosphate structure was confirmed by Rietveld analysis and the ^{27}Al, ^{31}P, and ^{19}F MAS NMR spectroscopy. The MAPA, located in the ten-membered ring channels, is doubly protonated to balance the negative charge of the $Al_3P_3O_{12}F_2^{2-}$ framework. Thermogravimetric analysis data have been used to study kinetics of the thermal decomposition of MAPA. The decomposition was found to be a complex process, its activation energy varied from 177 to 259 kJ mol^{-1}. The relatively high E values are explained by the fact that the MAPA cations are bound to the anionic framework both by electrostatic forces as well as strong N-H…O hydrogen bonds. The strength of the interactions is indirectly confirmed by the in situ high temperature X-ray diffraction analysis which shows that the MAPA decomposition leads to a phase transformation of the open-framework structure to the dense trydimite phase.

N. Rajic (✉) · D. Stojakovic · S. Jevtic
Faculty of Technology and Metallurgy, University of Belgrade, Belgrade 11000, Serbia
e-mail: nena@tmf.bg.ac.rs

N. Z. Logar · G. Mali · V. Kaucic
National Institute of Chemistry, Hajdrihova 19, Ljubljana 1000, Slovenia

Keywords Thermal degradation · Kinetics · Aluminophosphate · Porous · Open-framework · ULM-3

Introduction

Recently, we have reported kinetics of thermal degradation of 3-methylaminopropylamine (MAPA) captured inside the open-framework aluminophosphate $AlPO_4$-21 structure [1] and a layered zinc phosphate structure [2].

The MAPA exhibits a structure-directing role in the crystallization of these two phosphates by helping the metal-containing polyhedral and P-containing tetrahedral oxide units organize themselves into the unique structures. In the $AlPO_4$-21 structure, MAPA remains captured in the framework of eight-membered ring channels interacting with the framework oxygen atoms through a hydrogen bond network. In the layered zincophosphate structure MAPA is doubly protonated. It interacts with $[Zn_2P_3O_8(OH)_3]^{2-}$ macroanion not only through hydrogen bond network but also through strong electrostatic interactions. Thermal decomposition of MAPA in both phosphates starts above 573 K and occurs with a relatively high activation energy [1, 2]. In the $AlPO_4$-21, the decomposition is accompanied by a structural transformation without the loss of crystallinity, whereas in the layered zincophosphate the MAPA decomposition leads to a structural collapse.

Since, the fluoride ions together with organic amines can exhibit structure-directing function leading to crystallization of open-framework phosphates with unique structures [3], we have investigated, in the present study, the MAPA templating role in a fluoride medium.

Experimental

Synthesis

The synthesis was carried out hydrothermally in polytetrafluoroethylene-lined stainless-steel autoclaves. For the preparation of the reaction mixture, hydrated Al_2O_3 (77.8 wt%, Aldrich), orthophosphoric acid (85 wt%, Aldrich), 3-methylaminopropylamine (98 wt%, Fluka), HF (40 wt%, Merck), and H_2O were used in the following molar ratio: $0.5Al_2O_3$:H_3PO_4:0.5MAPA:HF:$100H_2O$. The mixture was homogenized using ULTRA TURRAX®, IKA® T18 basic stirrer. The initial pH was about 5.5 and it decreased to about 2 by the end of the reaction. The crystallization was performed at 433 K for 7 days. The obtained product (APOF) was filtered off, washed with distilled water and dried at 373 K.

Characterization techniques

Scanning electron microscope SUPRA 35 VP (Carl Zeiss) was used for examination of the crystal morphology. Elemental analysis was carried out using the energy dispersive X-ray spectroscopy (EDXS) analysis within Inca 400 (Oxford Instruments), attached to the scanning electron microscope SUPRA 35 VP.

The X-ray powder diffraction (XRPD) analysis was performed using a PANalytical X'Pert PRO diffractometer ($CuK_\alpha 1$ radiation, $\lambda = 1.54178$). The XRPD data were collected at room temperature in the 2Θ range from 5 to 60° in steps of 0.013° 2Θ with a total measuring time of 16 h. The qualitative powder analyses were carried out using Crystallographica Search-Match programs [4] and quantitative powder X-ray analysis using the Topas V2.1 Rietveld refinement program [5]. The high temperature X-ray diffraction (HTXRD) patterns were also collected on the PANalytical X'Pert PRO HTP diffractometer. The measurements were carried out at four different temperatures, i.e., at room temperature, at 573, 623, and 673 K.

NMR spectra were recorded on a 14.1T Varian Unity Inova spectrometer (3.2 mm MAS probehead) operating at 564.278, 156.289, and 242.800 MHz for the ^{19}F, ^{27}Al i ^{31}P, respectively. The sample was spun at a spinning rate of 12.5 kHz. The chemical shift axis for aluminum was referred to 1.0 mol dm^{-3} $Al(NO_3)_3$, to 85 wt% H_3PO_4 for phosphorus, and to $CFCl_3$ for the fluorine spectrum.

Thermal analysis was performed using a SDT Q-600 simultaneous DSC-TGA instrument (TA Instruments). The powdered samples (mass app. 10 mg) were heated in a standard alumina 90 µl sample pan. All experiments were carried out under air at a flow rate of 0.1 dm^3 min^{-1}. Non-isothermal measurements were conducted at heating rates of 1, 2, 4, 8, and 16 K min^{-1}. Five experiments were done at each heating rate. Isothermal experiments were carried out at temperatures in the range 593–673 K. A special heating program was used for isothermal measurements. The sample was isothermally heated at 523 K for 30 min to complete dehydration and then the temperature was increased at a heating rate of 20 K min^{-1} to the temperature at which the experiment was performed. Five experiments were undertaken at each chosen temperature.

Results and discussion

Hydrothermal crystallization yielded a white crystalline product (APOF). SEM analysis given in Fig. 1 shows that APOF crystallizes as white ball aggregates of a relatively uniform size of about 150 µm.

EDXS analysis gave a constant value of aluminum/phosphorous ratio over the whole ball. The ratio is 1:1 and its constant value indicates that APOF is a pure crystalline phase.

The X-ray diffraction pattern was successfully indexed giving an orthorhombic space group *Pbca* with the lattice parameters of $a = 9.9997(2)$ Å, $b = 18.1791(5)$ Å and $c = 15.8084(5)$ Å. Experimental conditions and crystallographic data are given in Table 1.

The crystallographic data are quite similar to those obtained earlier for the open-framework fluoroaluminophosphate [$Al_3(PO_4)_3F_2$, $H_3N(CH_2)_4NH_3$] [6], which is isotypic with the fluorogallophosphate structure-type ULM-3 [7, 8]. The aluminophosphate analog of ULM-3 prepared using 1,4-diaminobutane as the structure-directing agent crystallizes with a space group Pbc2(1) with cell parameters of $a = 10.023(2)$ Å, $b = 18.180(3)$ Å, and $c = 15.841(3)$ Å [6]. The 1,4-diaminobutane directs also the crystallization of fluoroferrophosphate analog of ULM-3 [9]. In all three structures the protonated amine resides in the ten-membered ring framework channels [6–9].

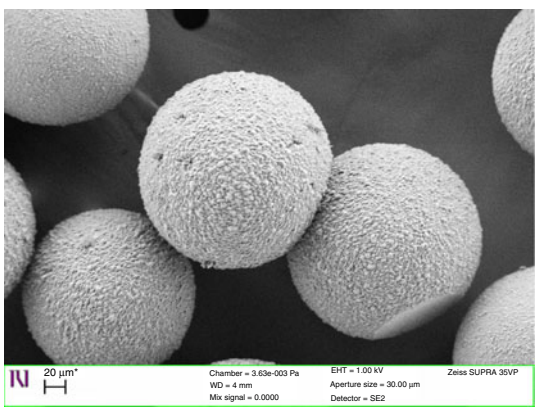

Fig. 1 A SEM photograph of APOF

Table 1 Experimental conditions and crystallographic data

Formula of the asymmetric unit	$Al_3P_3O_{12}F_2$, $C_4H_{14}N_2$
Crystal system	Orthorhombic
Unit cell dimensions	$a = 9.9997(2)$ Å
	$b = 18.1791(5)$ Å
	$c = 15.8084(5)$ Å
	$\alpha = 90^\circ$
	$\beta = 90^\circ$
	$\gamma = 90^\circ$
V/Å^3	2873.74(1)
Space group	*Pbca*
Dc/g Å^{-3}	1.3367(1)
T/K	293
λ/Å	1.5406 (Cu Kα_1)
Number of refined parameters	85
R_p	0.089
R_{wp}	0.197
R_{exp}	0.140

The inorganic framework of the APOF was derived using the structural data of ULM-3. The structure is built of the corner-linked $Al_3(PO_4)_3F_2$ units consisting of three PO_4 tetrahedra, two $AlPO_4F$ trigonal bipyramids, and one AlO_4F_2 octahedron. The three Al-containing polyhedra are linked through fluoride-bridges as shown in Fig. 2. The three-dimensional framework features ten-membered ring channels running along [100], which are interconnected with the eight-membered ring channels running along [101] and [10-1] directions.

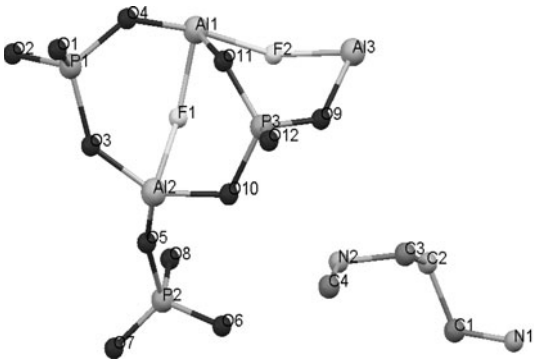

Fig. 2 Asymmetric unit of APOF with labeled atoms

One-dimensional ^{27}Al, ^{31}P, and ^{19}F MAS NMR spectra (Fig. 3) confirm the presence of three distinct aluminum, three distinct phosphorus, and two distinct fluorine sites in the asymmetric unit.

The MAPA is located in the ten-membered ring channels and is assumed to be doubly protonated in order to balance the negative charge of the $Al_3P_3O_{12}F_2^{2-}$ framework. Examination of the shortest N…O and N…F distances indicates the presence of strong hydrogen bonds between amine groups and the inorganic framework. The shortest N…O distance is found to be between 2.862 and 2.907 Å, whereas the N…F distance is 2.931 Å. It is worth mentioning that in $AlPO_4$-21 the MAPA species is captured inside an eight-membered ring channel system and is held to framework oxygen atoms by hydrogen bonds that correspond to somewhat longer N…O distances (2.914 and 2.985 Å).

TG analysis shows three main events between the room temperature and 973 K (Fig. 4). The first mass loss (about 2.5%) occurs between 473 and 573 K with a DTG maximum at about 493 K. This loss is attributed to the physically sorbed water. The second mass loss proceeds in a narrow temperature range between 623 and 673 K (18. 3%) with a DTG maximum at 653 K. It corresponds to the MAPA

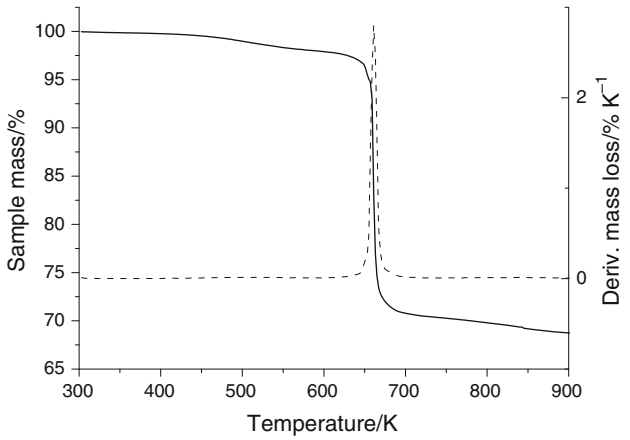

Fig. 4 TG (*solid line*) and DTG (*dashed line*) curves obtained at a heating rate of 20 K min^{-1}

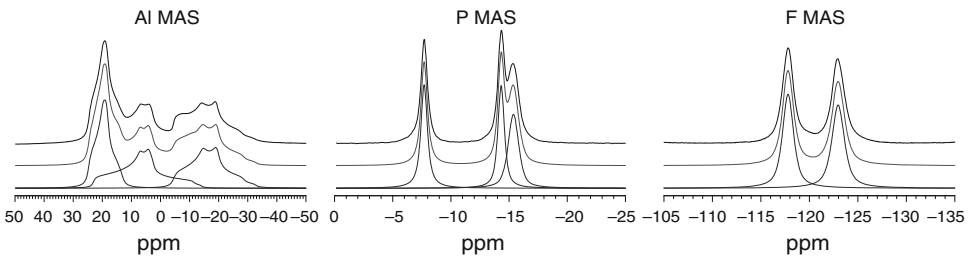

Fig. 3 ^{27}Al, ^{31}P and ^{19}F MAS NMR spectra of APOF. Experimental spectrum (*top line*) is compared to model (*middle line*) obtained as a sum of individual signals (*bottom lines*)

departure. The third loss, in the 673–973 K range, is related to the fluoride removal (7.5 wt%). The corresponding DTG maximum is at about 813 K.

The third mass loss is accompanied by a structural transformation of the open-framework structure to a dense tridymite phase as shown by the high temperature powder X-ray diffraction (Fig. 5).

The MAPA and fluoride thermal departures show an unexpected dependence on the heating rate as can be observed in the corresponding DTG profiles obtained under non-isothermal conditions (Fig. 6). It is seen that while the curves for the heating rates of 1 and 2 K min^{-1} exhibit a single broad maximum in the 573–673 K range, the curves obtained for 4 and 8 K min^{-1} show a splitting into two maxima. Moreover, the DTG curve for 16 K min^{-1} contains only one narrow asymmetric high intensity maximum. Such thermal behavior suggests that at different heating rates different kinetic processes take place. A possible reason for such behavior could be rather different temperature gradients between the surface and the interior of the sample particles at different heating rates. This is supported by the corresponding isothermal measurements, and the DTG curves differing considerably in shape at different temperatures in the 603–653 K range (Fig. 7).

In order to get an insight into the interaction of MAPA with the inorganic framework, we next used the DTG data in the 623–673 K range to estimate the average activation energies for the loss of MAPA at different decomposition degrees of MAPA. The procedure used was in accordance with the recommendations of the "ICTAC 2000 Project" [10]. Figure 8 shows the change of the reaction rates, $d\alpha/dt = \beta d\alpha/dT$ (α = conversion degree, t = time, β = heating rate, and T = temperature), with α for the heating rates of 1, 2, 4, and 8 K min^{-1}. The variation of the activation energy with α has

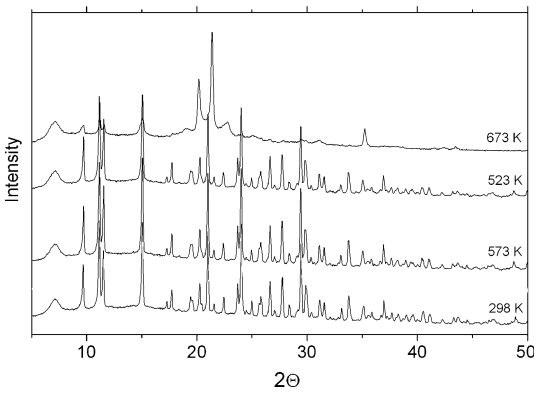

Fig. 5 XRD patterns obtained by in situ XRD analysis in the range of 298–673 K

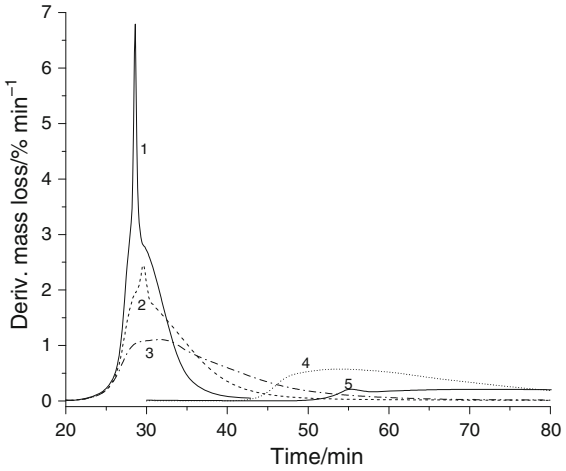

Fig. 7 DTG curves obtained under isothermal conditions at different temperatures: 653 K (*curve 1*), 643 K (*2*), 633 K (*3*), 623 K (*4*), and 613 K (*5*)

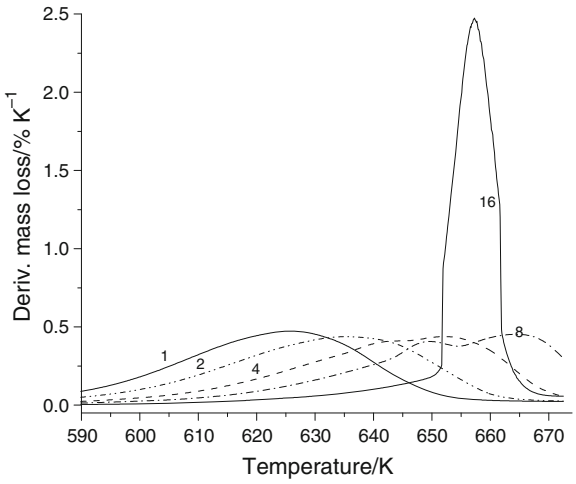

Fig. 6 DTG curves obtained at different heating rates; the numbers denote the heating rate (K min^{-1})

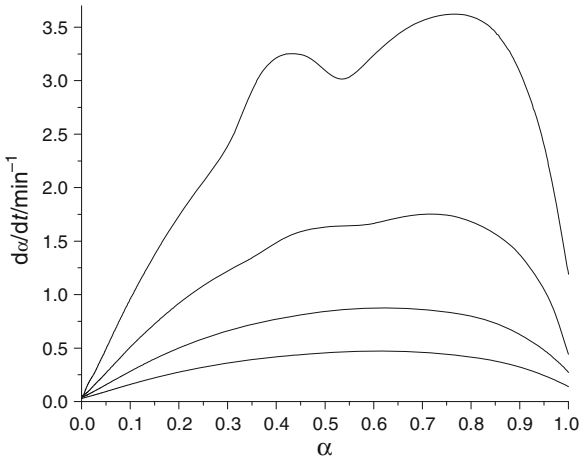

Fig. 8 Experimental reaction rates versus the conversion degree in the 623 to 673 K range for the MAPA loss from APOF. From the bottom up: heating rates of 1, 2, 4, and 8 K min^{-1}

Table 2 The activation energies (E/kJ mol^{-1}) obtained by Friedman's method for the data recorded at heating rates of 1, 2, 4, and 8 K min^{-1} (R is the correlation coefficient of the linear regression)

α	0.05	0.10	0.15	0.20	0.25	0.30	0.35	0.40	0.45	0.50	0.55	0.60	0.65	0.70	0.75	0.80	0.85	0.90	0.95
E	180	177	177	199	197	198	208	212.5	212	204	196	200	207	213	221	229.5	238.5	247	259
R	0.9931	0.9919	0.9933	0.9984	0.9985	0.9984	0.9973	0.9975	0.9983	0.9992	0.9993	0.9989	0.9990	0.9992	0.9992	0.9987	0.9981	0.9977	0.9969

been analyzed by the model-free isoconversional method of Friedman [11], described by the expression (1):

$$\ln\left(\frac{\mathrm{d}\alpha}{\mathrm{d}t}\right) = \ln\left(\beta\frac{\mathrm{d}\alpha}{\mathrm{d}t}\right) = \ln A + \ln[f(\alpha)] - \frac{E}{RT}\ldots\ldots \qquad (1)$$

For α = const., and using various heating rates (β), the plot of $\ln\left(\beta\frac{d\alpha}{dt}\right)$ versus $1/T$ should be linear and from the slope of the straight line the value of E is evaluated. The results obtained by such procedure from the data in Fig. 8 in the α range of 0.05 to 0.95 are shown in Table 2. (The data for 16 K min^{-1} were not included in the analysis; namely, due to narrowness of the corresponding maximum (cf. Fig. 6), the points corresponding to the 16 K min^{-1} data show large deviations from the straight line in the Friedman plots.)

Inspection of Table 2 shows that the loss of MAPA during the thermal treatment of APOF is characterized by a significant variation of the E value at different stages of the MAPA decomposition. The average E value is 209 kJ mol^{-1}, with E varying from 177 kJ mol^{-1} at $\alpha = 0.15$ to 259 kJ mol^{-1} at $\alpha = 0.95$. Such E variation of about 39% is yet another indication [12–15] that the loss of MAPA is a complex process (i.e., a multi-step reaction). The relatively high E values reflect the fact that the MAPA cations are bound to the anionic phosphate framework both by electrostatic forces as well as by strong N-H…O hydrogen bonds. Somewhat similar situation was found for a layered zinc phosphate where the diprotonated MAPA and the $[Zn_2P_3O_8(OH)_3]^{2-}$ layers are also bound together both electrostatically and by strong N-H…O bonds [2]. The MAPA decomposition here is a three-step process, the activation energy for the first step (343 kJ mol^{-1}) being even higher than for APOF. In contrast, in the $AlPO_4$-21 structure the MAPA and the inorganic lattice interact only through hydrogen bond network. The decomposition of MAPA in this case is characterized by a smaller activation energy (151–173 kJ mol^{-1} [1]), the decomposition being a single step reaction [1].

Conclusions

Both 3-methylpropylamine and fluoride ions exert a structure-directing role in the crystallization of the open-framework aluminophosphate analog of ULM-3. The fluorinated aluminophosphate lattice interacts strongly with 3-methylpropylamine which is evidenced by high values of the activation energy for the thermal decomposition of the captured amine. A rather large variation of the E value (from 177 to 259 kJ mol^{-1}) indicates that the latter decomposition is a complex process. Difference in thermal behavior of 3-methylpropylamine encapsulated in the aluminophosphate lattice and in the fluorinated aluminophosphate can be attributed to stronger interactions of amine with the fluorinated inorganic framework.

References

1. Dj Stojakovic, Rajic N, Jevtic S, Logar NZ, Kaucic V. A kinetic study of the thermal degradation of 3-methylaminopropylamine inside AlPO4–21. J. Therm. Anal. Calorim. 2007;87:337–41.
2. Rajic N, Logar NZ, Dj Stojakovic, Sajic S, Golobic A, Kaucic V. Hydrothermal synthesis and structure of a new layered zincophosphate intercalated with 3-methylaminopropylamine cations. J Serb. Soc. 2005;70:625–33.
3. Caullet P, Paillaud J, Simon-Masseron A, Soulard M, Patarin J. The fluoride route: a strategy to crystalline porous materials. C R Chimie. 2005;8:245–66.
4. Crystallographica Search-Match. Version 2.1.1.0: Oxford Cryosystems; 2003.
5. TOPAS V2.1. Users Manual. Karlsruhe: Bruker AXS; 2000.
6. Renaudin J, Loiseau T, Taulelle F, Ferey G. Synthesis and crystal structure of a fluoroaluminophosphate with open framework: $Al_3(PO_4)_3F_2$, N_2 C_4H_{14}. C R Acad. Sci. Paris Ser. IIb. 1996;323:545–53.
7. Loiseau T, Retoux R, Lacorre P, Ferey G. Oxyfluorinated microporous compounds: V. Synthesis and X-ray structural determination of ULM-3, a new fluorinated gallophosphate $Ga_3P_3O_{12}F_2$, $H_3N(CH_2)_3NH_3$, H_2O. J. Solid State Chem. 1994;111:427–36.
8. Loiseau T, Taulelle F, Ferey G. Oxyfluorinated compounds with open structure XI. Interaction between the ULM-3 type framework and linear diamine templates of different chain lengths studied by X-ray diffraction and solid/state nuclear magnetic resonance characterization. Microporous Mater. 1996;5:365–79.
9. Cavellec M, Riou D, Greneche J, Ferey G. Hydrothermal synthesis, structure and magnetic properties of $[Fe_3(PO_4)_3F_2$, $H_3N(CH_2)_4NH_3]$. J. Mag. Mag. Mater. 1996;163:173–83.
10. Brown ME, Maciejewski M, Vyazovkin S, Nomen R, Sempere J, Burnham A, et al. Computational aspects of kinetic analysis: Part A: the ICTAC kinetics project-data, methods and results. Thermochim. Acta. 2000;355:125–43.
11. Friedman HL. Kinetics of thermal degradation of char-forming plastics from thermogravimetry—Application to a phenolic plastic. J. Polym. Sci. 1965;6:183–95.
12. Budrugeac P, Popescu C, Segal E. Change of the apparent reaction order with temperature as a consequence of the reaction mechanism complexity. J. Therm. Anal. Calorim. 2001;64:821–7.
13. Budrugeac P. Some methodological problems concerning the kinetic analysis of non-isothermal data for thermal and thermo-oxidative degradation of polymers and polymeric materials. Polym. Degrad. Stab. 2005;89:265–73.
14. Vlase T, Vlase G, Doca N. Thermal stability of food additives of glutamate and benzoate type. J. Therm. Anal. Calorim. 2005;80:425–8.
15. Budrugeac P, Homentcovschi D, Segal E. Critical analysis of the isoconversional methods for evaluating the activation energy. I. Theoretical background. J. Therm. Anal. Calorim. 2001;63:457–63.